

Structural, Phase Transition, Morphological, Optical and Dielectric Properties of Lead Free $(1-x)(\text{Na}_{0.99}\text{K}_{0.01})(\text{Nb}_{0.95}\text{Sb}_{0.05})\text{O}_3-x\text{BaTiO}_3$ Solid Solutions

S. Sasikumar, S. Saravanakumar, S. Asath Bahadur, T.K. Thirumalaisamy

Abstract: In this work, lead free $(1-x)(\text{Na}_{0.99}\text{K}_{0.01})(\text{Nb}_{0.95}\text{Sb}_{0.05})\text{O}_3-x\text{BaTiO}_3$, where $x=0.1, 0.2$ ceramic solid solution systems were prepared via solid state sintering method. X-ray diffraction (XRD) reveals that the influence of Ba^{2+} on crystal structure of the NKNS-xBT ($x=0.1, 0.2$) solid solutions. PXRD analysis showed that Ba^{2+} addition into NKNS ceramics caused significant change in crystal symmetry from tetragonal to cubic. The surface morphology of the prepared ceramics were determined by scanning electron microscopic (SEM) measurements and revealed that the uniform distribution of grains. Energy band gap were determined by UV-visible absorption spectrophotometer. Dielectric measurements show the maximum dielectric constant ($\epsilon \sim 3044$) and temperature ($T_m \sim 120^\circ\text{C}$) at 1 kHz.

Keywords : Ceramics, scanning electron microscopy, phase transition, dielectric properties, optical properties.

I. INTRODUCTION

The $\text{Pb}(\text{Zr}, \text{Ti})\text{O}_3$ related perovskites have excellent ferroelectric and dielectric properties with higher Curie temperature (TC) and are applied in transducers, sensors, actuators and buzzers [1]. The lead-based ceramics increase more environmental problems due to the toxicity, which produce toxic lead oxide (PbO) during the preparation through evaporation [2,3]. To overcome the environmental problems, in the search of new ceramic materials, the extensive reports on lead free based ceramics were conducted. $\text{Na}_{0.5}\text{K}_{0.5}\text{NbO}_3$ based ceramics and BaTiO_3 based piezoceramics considered as promising candidates because of good electrical properties and environmentally harmless [4-7].

Revised Manuscript Received on December 16, 2019.

* Correspondence Author

S. Sasikumar, Department of Physics, International Research centre, Kalasalingam Academy of Research and Education, Krishnankoil -626126, Tamil Nadu, India. Email: sasikuhan@gmail.com

S. Saravanakumar, Department of Physics, International Research centre, Kalasalingam Academy of Research and Education, Krishnankoil -626126, Tamil Nadu, India. Email: saravanaphysics@gmail.com

S. Asath Bahadur*, Department of Physics, International Research centre, Kalasalingam Academy of Research and Education, Krishnankoil -626126, Tamil Nadu, India. Email: s.asathbahadur@klu.ac.in

T.K. Thirumalaisamy, Department of Physics, Hajee Karutha Rowther Howdia College, Uthamapalayam - 625 533, Tamil Nadu, India. Email: tktsamy67@gmail.com

However, NKN based ceramics are difficult to obtain dense. Evaporation of the sodium and potassium ions during the heating causes the deviation of compositional stoichiometry. Therefore, it is a necessary to enhance the electric properties of $\text{Na}_{0.5}\text{K}_{0.5}\text{NbO}_3$ based solid solutions by the aids, such as BaTiO_3 , $\text{K}_{0.5}\text{Bi}_{0.5}\text{TiO}_3$ and etc. [8,9]. BaTiO_3 has been widely used as capacitors, sensors and actuators and memory storage devices due to the superior dielectric, ferroelectric and piezoelectric properties, with high sintering temperature and low Curie temperature [10-12].

In this study, we fabricated NKNS-xBT, ($x=0.1, 0.2$) solid solutions to study how the doping influences the structural properties. So, this report primarily aims to analyze the structural properties by Rietveld analysis [13] of XRD profiles of the NKNS-xBT ceramics. In this present work, the ceramic solid solutions were successfully synthesized via solid state sintering process and structure, morphological, optical and dielectric properties were successfully investigated.

II. EXPERIMENTAL

A. Materials synthesis

Polycrystalline samples of $(1-x)(\text{Na}_{0.99}\text{K}_{0.01})(\text{Nb}_{0.95}\text{Sb}_{0.05})\text{O}_3-x\text{BaTiO}_3$, ($x=0.1, 0.2$) solid solution systems were synthesized using solid state sintering process. The raw starting chemicals were carefully weighed with their molar ratio of the molecular formula and Na_2CO_3 , K_2CO_3 , Nb_2O_5 , Sb_2O_3 , BaCO_3 and TiO_2 are used as starting materials (Alfa-Aesar). The weighed oxide and carbonate chemicals were mixed using mortar and pestle followed by calcined for 1000°C for 4 h. The decarbonated mixtures were again ground using mortar and pestle for 5 h. Before sintering, the powders were pelletized with stainless steel die of 12 mm dia and 1-2 mm thickness. Then, the pressed discs were sintered at 1200°C for 2 h using tubular programmable furnace.

B. Materials characterization

The purity of the crystalline structures were analyzed by X-ray diffractometer (Burker,

Structural, Phase Transition, Morphological, Optical and Dielectric Properties of Lead Free (1-x)(Na_{0.99}K_{0.01})(Nb_{0.95}Sb_{0.05})O₃-xBaTiO₃ Solid Solutions

Karlsruhe, Germany) with CuK α radiation ($\lambda=1.54056 \text{ \AA}$) with the range of diffraction angle $2\theta=10^\circ-120^\circ$ with a step of 0.02° . Structural profile refinement was performed by the Rietveld refinement [13] method through JANA2006 [14] software. Microstructure and elemental analysis were performed by scanning electron microscopic technique and energy dispersive X-ray spectroscopy (Zeiss-EVO 18 Research) respectively. Optical properties were analyzed by UV-visible absorption spectra using Varian, Cary 5000 spectrophotometer (wavelength range 200-800 nm). Temperature dependence of dielectric measurements was recorded by impedance dielectric spectrometer (PSM 1735, N4L) for various frequencies. Before dielectric measurements, sintered pellets were painted by silver paste on the surfaces.

III. RESULTS AND DISCUSSION

A. XRD and Rietveld profile refinement analysis

Fig. 1 depicts the X-ray diffraction profiles of NKNS-xBT, ($x=0.1, 0.2$) ceramics. The peaks are well defined and indexed (001), (110), (200), (211) peaks. The PXRD data sets confirm that the diffraction peaks assigned to tetragonal structure ($x=0.1$) with $P4mm$ space group confirmed by the standard data (JCPDS file no. 05-0626). The diffraction peaks corresponding to the perovskite structure for $x=0.2$ confirmed by cubic. The (110) diffraction peak shifted towards the lower diffraction angle of 2θ as Ba^{2+} concentration increased. This due to fact that the higher ionic radius of Ba^{2+} (ionic radius: 1.34 \AA) with respect to relative ionic radius of Na^+ and K^+ (ionic radius: 0.97 \AA and 1.33 \AA) in the matrix [15]. The tetragonal distortion (c/a) is found to 1.005 for $x=0.1$, and 1 for $x=0.2$ as shown in Table 1. There is a structural phase transition from tetragonal ($P4mm$) to cubic ($Pm-3m$) structures of the unit cell is evidenced with increasing Ba^{2+} content.

In order to find more information about crystal structure, the Rietveld refinement has been performed using JANA2006 [14] software by the PXRD data. The fitted profiles of samples with $x=0.1$ and 0.2 compositions are presented in figs. 2 (a) and (b). The refined profile results showed that the acceptable R-factors such as R_p , R_{obs} were extracted from profile refinement results and all parameters are given in table 1. From the Rietveld refinement [13], it is noticed that the cell parameters increases while increasing Ba^{2+} substitution. The average crystallite size was calculated for the compositions using Debye-Scherrer's formula, [16],

$$D = \frac{0.9\lambda}{\beta \cos \theta} \quad (1)$$

where β is FWHM (width at half maximum of the peak), λ is wavelength of CuK α radiation and θ is the Bragg angle. The calculated average crystallite size (D) values listed in Table I.

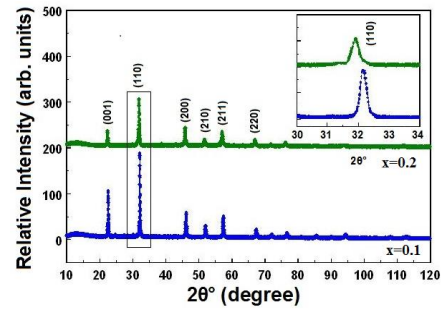


Fig. 1.(a) Powder XRD patterns of NKNS-xBT, ($x=0.1, 0.2$) solid solutions, inset shows the magnified view of (110) peak.

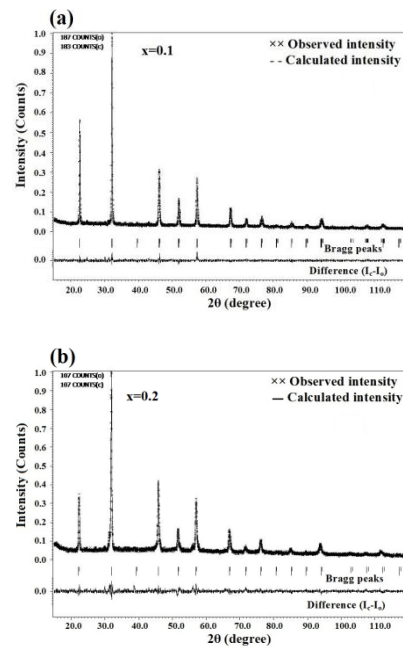


Fig. 2. Fitted X-ray profiles for NKNS-xBT, a) $x = 0.1$, b) $x = 0.2$.

Table-I: Structural parameters of NKNS-xBT

Parameters	$x = 0.1$	$x = 0.2$
$a = b$ (\AA)	3.9250 (14)	3.9562(6)
c (\AA)	3.9587(13)	3.9562(6)
c/a	1.008	1.002
Space group	$P4mm$	$Pm\ m$
Volume (\AA^3)	60.99(4)	61.43 (1)
Density (gm/cc)	4.47(3)	4.43 (1)
R_p (%)	5.97	7.06
R_{obs} (%)	2.12	3.49
GOF	0.20	0.22
$F_{(000)}$	76	76
Crystallite size(nm)	77	30

B. Surface morphology and EDS analysis

Figs. 3 (a) and (b) show the surface morphology images of NKNS-xBT, ($x=0.1, 0.2$) ceramics measured by scanning electron microscopy. All ceramics appear square shaped particles. The EDS spectra



reveals that the elemental compositions of the solid solution systems. The spectra revealed that only expected elements, are present in NKNS-xBT, (x=0.1, 0.2) ceramics, no traces of other elements were detected in the EDS spectra. The EDS spectra NKNS-xBT, (x=0.1, 0.2) solid solution ceramics are shown in figs. 3 (c) and (d). The percentages of atomic and weight content of elements present in the ceramic solid solutions are given in Table II.

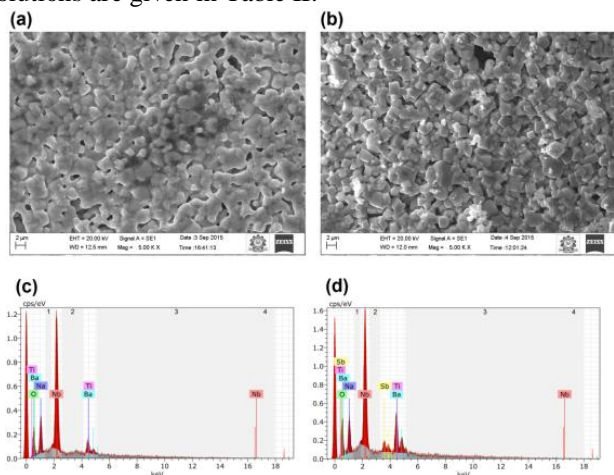


Fig. 3. SEM images of NKNS-xBT for a) x = 0.1, b) x = 0.2 and EDS spectra of NKNS-xBT, c) x = 0.1, d) x = 0.2

Table-II: Elemental compositions of NKNS-xBT (x=0.1, 0.2) ceramics

Sample	Weight (wt. %)						
	Na	K	Nb	Ba	Ti	Sb	O
x=0.1	13.1 3	0.52	45.3 6	11.1 3	1.28	0.67	27.91
x=0.2	13.0 6	0.77	47.1 0	9.37	1.51	0.69	28.51
	Atomic (At. %)						
	Na	K	Nb	Ba	Ti	Sb	O
x=0.1	19.5 8	0.66	16.0 9	2.75	0.91	0.75	59.30
x=0.2	18.8 7	1.36	16.7 0	2.31	1.07	0.71	60.33

C. Optical properties of NKNS-xBT ceramics

In order to analyze the band gap energy of ceramics, the absorbance spectra versus wavelength were measured from 200-800 nm. Fig. 4 indicates the absorption spectrum of the solid solutions. It reveals a strong absorbance peak at 314 nm. The energy band gap (E_g) values can be evaluated by Tauc relation [17] as: $\alpha h\nu = A(h\nu - E_{gap})^n$, where E_{gap} is band gap energy, A is proportionality parameter, α is absorption coefficient, ν is frequency, h is plank constant and n consider as 1/2 for direct allowed transition. From the Tauc plot (Fig. 5), a clear displacement has been noticed and energy band gap values for x=0.1 is 3.294 eV and x=0.2 is 3.314 eV, respectively. The estimated optical band gap values of solid solutions noted in Table III.

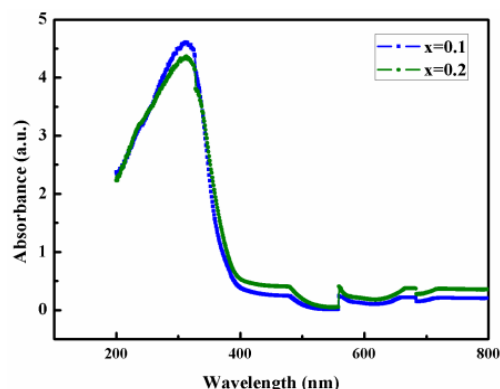


Fig. 4. UV-visible absorption spectra of NKNS-xBT, (x=0.1, 0.2) ceramics

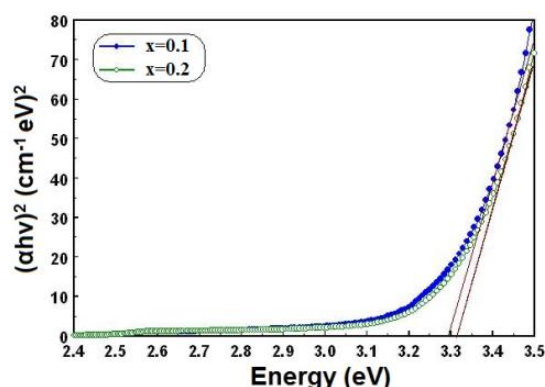


Fig. 5. Tauc plot for NKNS-xBT, (x=0.1, 0.2) solid solutions

Table-III: Band gap of NKNS-xBT, (x=0.1, 0.2) ceramics

Samples	Energy gap (eV)	Wavelength (nm)
x = 0.1	3.294	314
x = 0.2	3.314	314

D. Dielectric properties of NKNS-xBT ceramics

Fig. 6 displays temperature dependent dielectric constant (ϵ) of ceramics measured up to 250°C at various frequencies (1, 10, 100 kHz and 1 MHz). The effect of Ba²⁺ substitutions on the dielectric behaviour of ceramics shows the dielectric peak around 120°C, indicating that the Curie temperature (T_C) for x=0.1 sample. Based on literature [18], the sodium potassium niobate-barium titanate presents the Curie temperature ($T_C \sim 110$ K). The transition temperature (T_C) of solid solution shifted towards lower temperature for x=0.2 composition. It can be seen that the composition x=0.1 has the higher dielectric constant ($\epsilon \sim 3044$) at frequency of 1 kHz, due to the ferroelectric tetragonal phase. With further increasing x, the T_C decreases to room temperature, due to phase transition of ferroelectric to paraelectric phase. The dielectric constant values of NKNS-xBT (x=0.1, 0.2) ceramics are given in Table IV at 1 kHz.

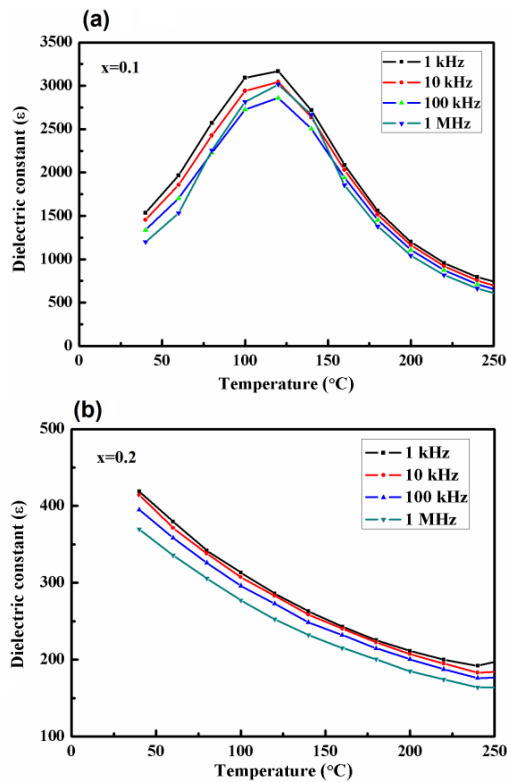


Fig. 6. Dielectric property of NKNS-xBT ceramics, a) x=0.1, b) 0.2

Table-IV: Dielectric parameters of NKNS-xBT, (x=0.1, 0.2)

Samples	ε
x=0.1	3044
x=0.2	407

IV. CONCLUSION

Polycrystalline ceramics of NKNS-xBT, (x=0.1, 0.2) ceramics were prepared using solid state sintering method. The XRD studies confirm pure perovskite structure with single phase. With an increase of Ba concentration, NKNS-xBT, (x=0.1, 0.2) samples show the structural transformation from tetragonal to cubic structure revealed by PXRD. The SEM analyses indicate that the samples are uniform surface morphology. The EDS results confirm the presence of elements in the solid solutions close to the expected proportion. From UV-Visible spectra, it was observed that E_{gap} value decreased when the addition of Ba concentration. The dielectric responses as a function of temperature showed that the Ba substitution in NKNS affects the transition temperature by shifting to a lower temperature, consistent with the ferroelectric and XRD studies transformed paraelectric nature.

ACKNOWLEDGEMENT

The author S. Sasikumar is grateful thank to Kalasalingam Academy of Research and Education, Krishnankoil for recognition and providing financial support as the Post Doctoral Research Fellowship.

REFERENCES

1. N. Setter, Piezoelectric Materials in Devices. EPFL Swiss Federal Institute of Technology; Lausanne, Switzerland: 2002.
2. B. Malic, A. Bencan, T. Rojac, M. Kosec, Lead-free piezoelectrics based on alkaline niobates: Synthesis, sintering and microstructure. Acta Chim. Slov. vol. 55, pp.719-726, 2008.
3. C. Fujioka, R. Aoyama, H. Takeda, and S. Okamura, J. Eur. Ceram. Soc., vol. 25, pp. 2723, 2005.
4. R.J. Xie, Y. Akimune, R. Wang, N. Hirisaki, and T. Nishimura, Jpn. J. Appl. Phys. vol. 42, pp. 7404, 2003.
5. I.H. Im and K. H. Chung, J. Nanosci. Nanotechnol, vol. 14, pp. 8920, 2014.
6. R.Z. Zuo, X.S. Fang, and C. Ye, Appl. Phys. Lett, vol. 90, pp. 092904, 2007.
7. S. G. Bae, H.G. Shin, E.Y. Sohn, and I.H. Im, Trans. Electr. Electron. Mater, vol. 14, pp. 78, 2013.
8. Y. Saito, H. Takao, T. Tani, T. Nonoyama, K. Takatori, T. Homma, T. Nagaya, Nature, vol. 432, pp. 84, 2004.
9. S.H. Lee, K.S. Lee, J.H. Yoo, Y. H. Jeong, H. S. Yoon, Trans. Electr. Electron. Mater, vol. 12, pp. 72, 2011. T. Okamoto, S. Kitagawa, N. Inoue, A. Ando, Appl. Phys. Lett., vol. 98, pp. 072905, 2011.
10. S.-C. Huang, H.-M. Chen, S.C. Wu, J.Y.-M. Lee, J. Appl. Phys. vol. 84, pp. 5155-5157, 1998.
11. A.A. Heitmann, G.A. Rossetti, Jr, Integr. Ferroelectr, vol. 126, pp.155-165, 2011.
12. H.M. Rietveld, J. Appl. Crystallogr. Vol. 2(2), 6, 1969.
13. V. Petricek, M. Dusek, L. Palatinus, Zeitschrift fur Kristallographie, vol. 229(5), pp. 345-352, 2014.
14. R.D. Shannon, Acta Crystallogr. Sect, vol. A32, pp. 751, 1976.
15. S. Saravanakumar, R. Saravanan, S. Sasikumar, Chem. Pap., vol. 68(6), pp. 788-707, 2014.
16. D.L. Wood, J. Tauc, Phys. Rev B. vol. 5(8), pp. 3144, 1972.
17. J. Zeng, L. Zheng, G. Li, Z. Cao, K. Zhao, Q. Yin, E.D. Politova, J. Alloy. Compd., vol. 509, pp. 5858-5862, 2011.

AUTHORS PROFILE



S. Sasikumar received his Ph.D degree in 2018 at Madurai Kamaraj University, India. He has expertise in the area of piezoelectric applications. He has published 19 peer reviewed research articles in international Journal with 56 citations.



S. Saravanakumar received his Ph.D. degree in 2015 at Madurai Kamaraj University, India. He is expertise in the areas of spintronics materials and the structural and magnetic properties of semiconducting material. He has published 26 peer reviewed research articles in international Journals with over 107 citations.



Dr. S. Asath Bahadur is a Senior Professor in the Department of Physics, School of Advanced Sciences at Kalasalingam Academy of Research and Education, India. He has obtained Ph.D. in the area of X-ray crystallography from Madurai Kamaraj University in 1994. He has expertise in the areas of Crystallography and Material science. He has published more than eighty five peer-review research articles in journals of international repute besides seventy more as proceedings.



T.K. Thirumalaisamy received his Ph.D degree in 2018 at Madurai Kamaraj University, India. He has expertise in the area of applications of Non linear optical materials. He has published 8 peer reviewed research articles in international Journal with 10 citations.